

M.L. RICHARDS, U. SCHMUCKER and E. STEVELING

"Magnetic variations and magnetotelluric studies in Rheingraben and Schwarzwald"

Magnetotelluric and magnetovariational surveys were made in 1977/78 along two east-west oriented profiles from the Rheingraben to the Schwäbische Alb, crossing the Schwarzwald in the north by Baden-Baden and in the south by Freiburg. The aim was to test equipment and analysis methods in the context of a geothermal resources program. Most of the data have been analysed and some results of magnetotelluric analysis are described in the following.

The aim of instrumentation and digital data recorder design was to cover at least the two frequency ranges for pulsations and polar substorms (SCHMUCKER, et. al., 1980). Induction coil magnetometer is used in the former range, and either fluxgate or Askania variometer for the latter. The telluric apparatus incorporates Ag-AgCl electrodes.

The area of the survey is shown in Fig. 1, where the stations to be discussed are underlined. The electric field was measured for only 1 or 2 days at each of stations BAD, ENZ, NBU, ENT, KOH and TIE, and long period magnetic field was not

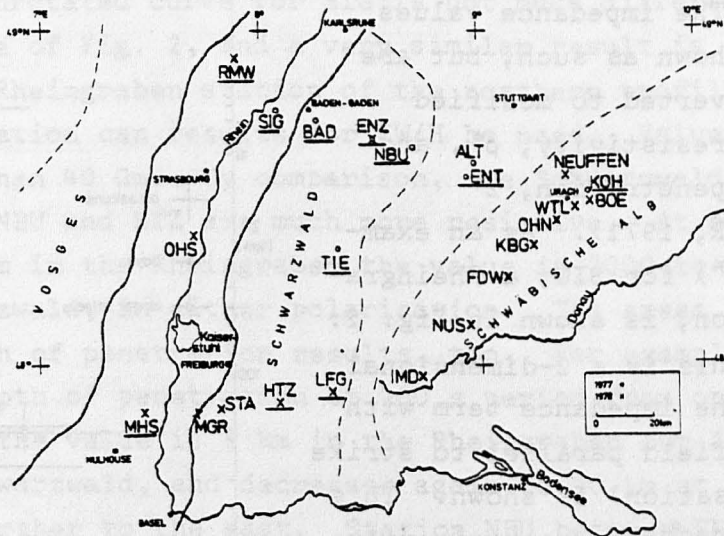


Fig. 1: Station locations; those underlined are discussed in the text.

measured at LFG. So there are bay-period results only at RMW, SIG, ALT and HTZ. For the 3 stations ENZ, NBU and TIE, however, the pulsation data were filtered and decimated, and longer effects selected to extend the results to 2000 s period. Longer period pulsation effects were also analysed at HTZ, as well as bays, and effectively bridge the gap between bays and pulsations.

Data analysis follows SCHMUCKER (1978). Selected data segments are filtered and decimated as required and then Fourier transformed. Smooth estimates of spectra and cross spectra at selected frequencies are obtained by first, convoluting the raw spectra with a Parzen spectral window, and second, averaging these values over the available effects. Typical window widths are between 0.05 and 1.0 cph for the frequency range 0.05 to 8.0 cph, and between 0.6 and 96.0 cph for the range 1.8 to 480.0 cph. One variation of this scheme was to use a cosine data window for pulsation effects.

The impedance function (and its error) that is used for the magnetotelluric interpretation is calculated from the smooth spectra values. The off-diagonal elements of the impedance tensor, corresponding to the N-S electric component response to D magnetic variations, and E-W elec-

tric to H magnetic, are later called NS/D and EW/H, respectively. The impedance values are not shown as such, but are first converted to modified apparent resistivity,  $\rho^*$ , and depth of penetration,  $z^*$  (SCHMUCKER, 1971). As an example,  $\rho^*(z^*)$  for SIG, a Rheingraben station, is shown in Fig. 2. Because this is a 2-dimensional feature the impedance term with electric field parallel to strike (E-polarisation) is shown. This is about N20E, or approximately the NS/D polarisation. The bars express the error estimate, and the frequency is noted alongside.

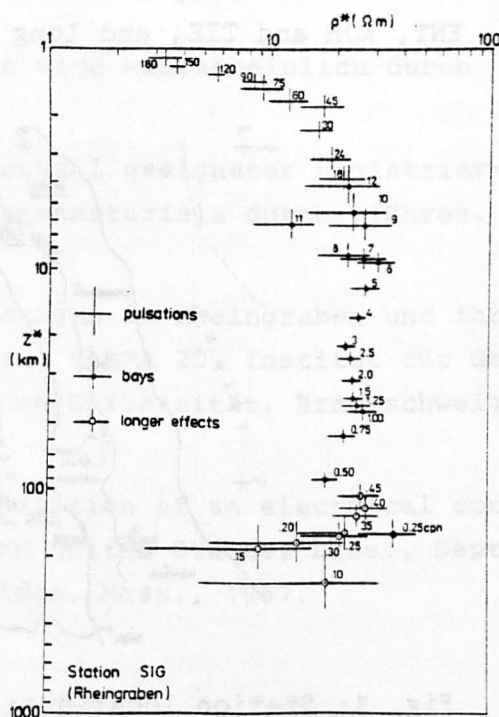


Fig. 2: SIG, E-polarisation.

For depths  $1 < z^* < 4$  km the results are from pulsation analysis in the period range 20 to 200 s; values for  $5 < z^* < 105$  km are for bay effects with period range 5 min to 4 h. Maximum depths of penetration are obtained for "longer effects", which are storm-time segments that are long enough to allow analysis at periods from 2 to 10 h.

In the upper few km  $\rho^*$  increases smoothly from 3 to 30  $\Omega\text{m}$ . This is the signature of the graben sediment fill which from concurrent evidence has a conductance of 1000 to 1500 S at this location. The value of  $\rho^*$  remains between 15 and 35  $\Omega\text{m}$  for  $3 < z^* < 200$  km, with a slight decrease at 20 km and a tendency to smaller value at the greatest depths of penetration.

A summary of results for all the stations marked in Fig. 1 is presented in Fig. 3. Coordinates are not rotated in this case, and in both parts 'a' and 'b' the upper and lower panels are for NS/D and EW/H polarisations, respectively. Fig. 3a is for the northern profile and 3b for the southern. Individual estimates are not given, except for those at periods 20, 200 and 2000 s. The dashed curves are smoothed representations of  $\rho^*(z^*)$ , and error bounds are indicated by the solid lines. Note that the log  $z^*$  scale is the same for each station, but the log  $\rho^*$  scale ranges over low values for RMW and SIG and high values for all the others.

The unrotated curve for SIG is not much different from the rotated one of Fig. 2, and a very similar result is seen at RMW, the other Rheingraben station of the northern profile. For neither station can results for EW/H be used. Values of  $\rho^*(z^*)$  are less than 40  $\Omega\text{m}$ . By comparison, the Schwarzwald stations BAD, ENZ, NBU and HTZ are much more resistive. At depths where  $\rho^*$  is 30  $\Omega\text{m}$  in the Rheingraben the value is 2000 to 3000  $\Omega\text{m}$  in the Schwarzwald, in either polarisation. The areas are contrasted in depth of penetration results, too. For example, following the depth of penetration at 200 s period from one curve to the next, the value is 5 km in the Rheingraben but 100 to 200 km in the Schwarzwald, and decreases again to 40 km at stations ENT and KOH further to the east. Station NBU between ENZ and ENT appears to be transitional in both polarisations, but at BAD the result is about the same as at ENZ in NS/D polarisation. However, the impedance is isotropic at ENZ and not at BAD,

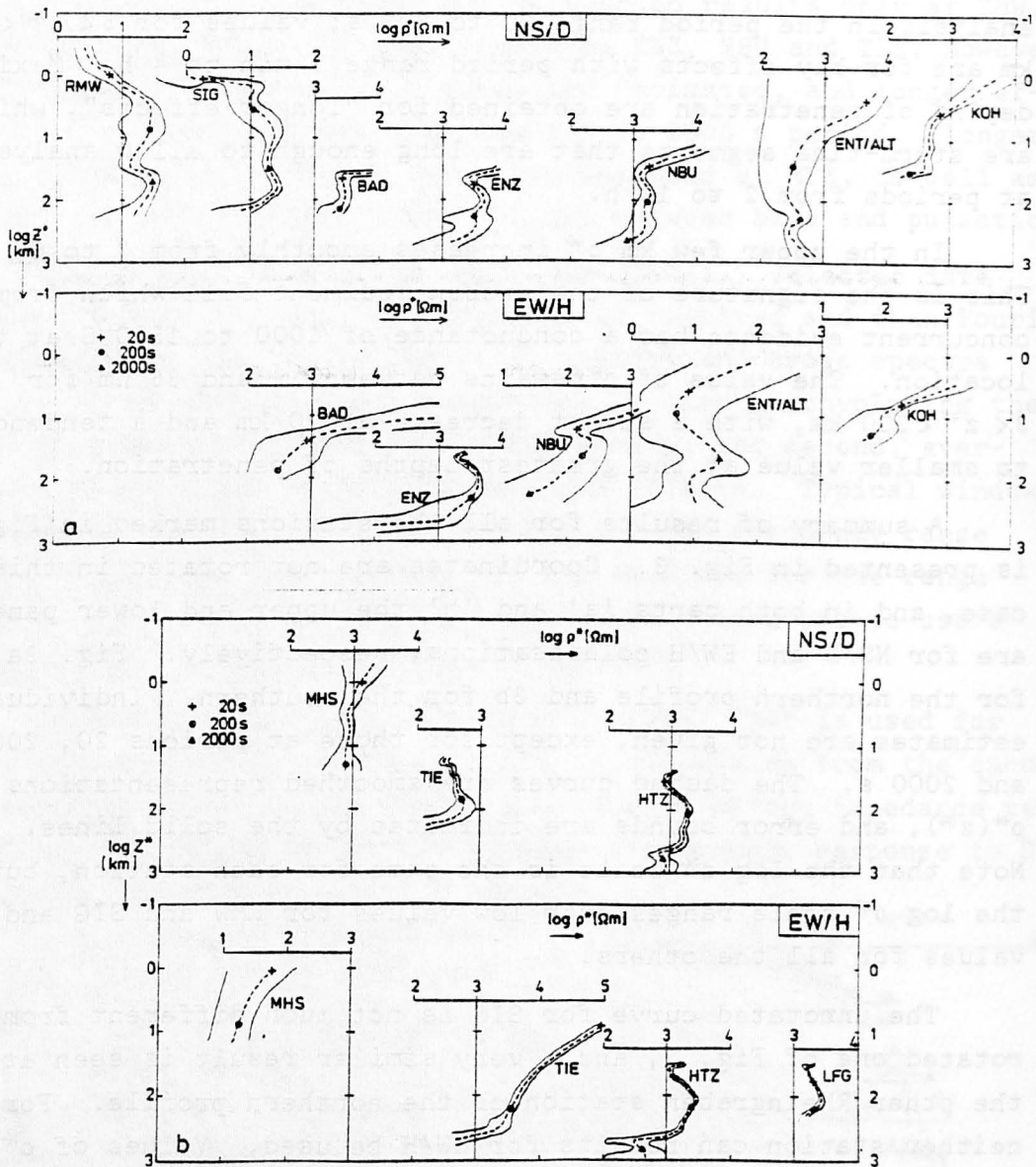


Fig. 3:  $\rho^*(z^*)$ , unrotated impedance, for stations indicated in Fig. 1.

clearly indicating the influence of the graben.

A second representation of station resistivity structure is obtained by use of an inverse, one-dimensional model algorithm (SCHMUCKER, 1974). Starting with the E-polarisation impedance element, including errors, models with different constraints were found for stations RMW, SIG and HTZ. The simplest realistic model is two layers over a halfspace. Increasing this to 3 layers makes a small improvement, and these results of the inversion algorithm are shown in Fig. 4.

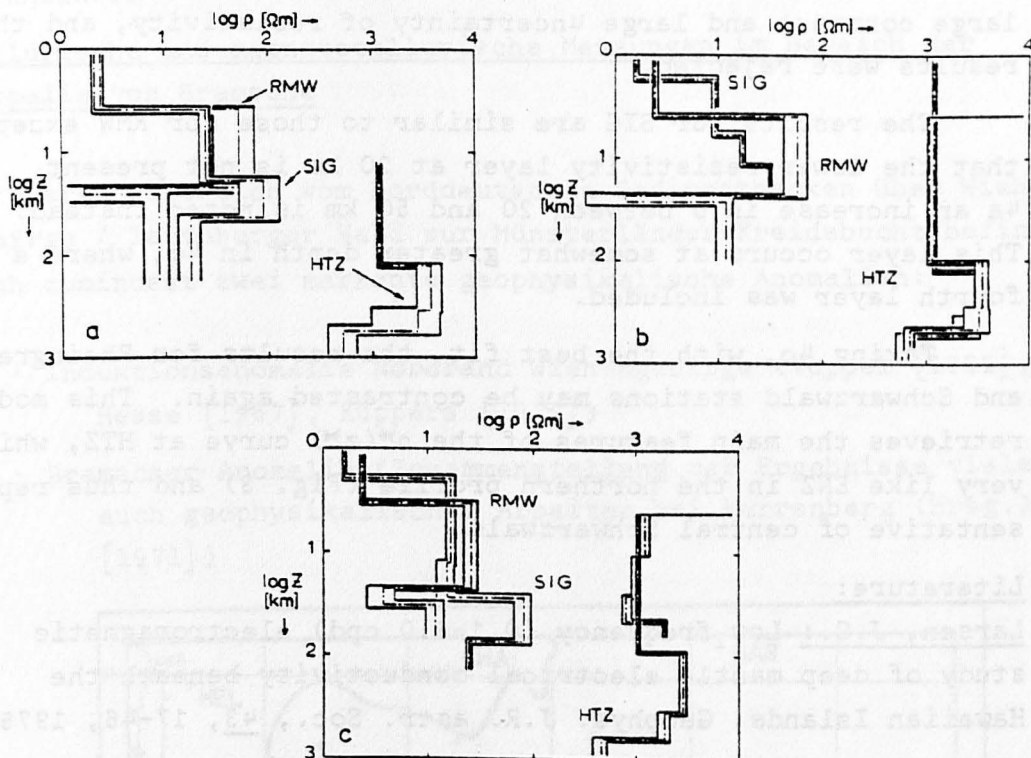


Fig. 4: One-dimensional models.

In 4b and 4c the data are weighted inversely by the data errors; in 4a no weighting was used. For cases 4a and 4b the product of conductivity times thickness squared is constant in each layer, but in 4c this product is weighted linearly, with smaller weights for the upper layers (LARSEN, 1975).

For RMW and HTZ the results are not essentially different in the 3 cases, although for RMW the low resistivity at about 20 km depth is more clearly resolved when both data variance and layer weighting are employed. The change in HTZ model when, in 4b, the effect of a nonconducting layer of 50 km thickness is removed before the inversion is a modest (25 km) shallowing of the more resistive layer. This nonconductor is present in case 4c also, where two models for HTZ are shown; both show features of the  $\rho^*(z^*)$  curve in Fig. 3, but the one with deeper structure has the smaller fitting error,  $\epsilon$ .

The error  $\epsilon$  systematically decreases from 4a to 4b to 4c. Increasing the number of layers also reduces  $\epsilon$ , but the effect is to introduce alternating resistive and conductive layers of

large contrast and large uncertainty of resistivity, and these results were rejected.

The results for SIG are similar to those for RMW except that the lower resistivity layer at 20 km is not present. In 4a an increase in  $\rho$  between 20 and 50 km is noted instead. This layer occurs at somewhat greater depth in 4c, where a fourth layer was included.

Taking 4c, with the best fit, the results for Rheingraben and Schwarzwald stations may be contrasted again. This model retrieves the main features of the  $\rho^*(z^*)$  curve at HTZ, which is very like ENZ in the northern profile (Fig. 3) and thus representative of central Schwarzwald.

Literature:

Larsen, J.C.: Low frequency (0.1-6.0 cpd) electromagnetic study of deep mantle electrical conductivity beneath the Hawaiian Islands. Geophys. J.R. astr. Soc., 43, 17-46, 1975.

Schmucker, U.: Neue Rechenmethoden zur Tiefensondierung. Protokoll Erdmagnetische Tiefensondierung, Rothenberge/Westf., 1-39, 1971.

Schmucker, U.: Erdmagnetische und magnetotellurische Sondierungen mit langperiodischen Variationen. Protokoll Erdmagnetische Tiefensondierung, Grafrath/Bayern, 313-342, 1974.

Schmucker, U.: Auswertungsverfahren Göttingen. Protokoll Elektromagn. Tiefenforschung, Neustadt/Weinstraße, 163-188, 1978.

Schmucker, U., M.L. Richards, E. Steveling, J. Watermann: Erdmagnetische und magnetotellurische Sondierungen im Gebiet des mitteleuropäischen Riftsystems. Schlußbericht EG (126-76EGD und 317-77-11EGD), Inst. f. Geophysik d. Univ. Göttingen, 1980.